Antenna Coupling Effects for Space-Time Radar Waveforms: Analysis and Calibration

Galina Babur, Pascal J. Aubry, and François Le Chevalier

***Abstract*—In this paper, we investigate the impact of mutual coupling between the antenna array elements on the performance of a multiple-input multiple-output (MIMO) radar with colored waveform transmission (collocated coherent MIMO system). Simulation results confirm the decrease in system performance when antenna mutual coupling is taken into account. A dedicated scan-dependent calibration technique is proposed for elimination of the coupling effect. The experiments with a real X-band antenna array validate the coupling analysis and the calibration procedure presented in this paper.**

***Index Terms*—Antenna coupling effects, coherent multiple-input multiple-output (MIMO), signal processing, space-time waveforms.**

I. Introduction

MULTIPLE-INPUT multiple-output (MIMO) radars enhance performance by transmitting and receiving coded waveforms from multiple locations [1], [2]. Orthogonality of the transmitted waveforms is a requirement for allowing separation at the receiver. In addition, the use of signals with large BT-product (e.g., coded signals) on transmit to achieve pulse compression can be particularly effective in improving target detection capability by radiation of a larger amount of average radar power without exceeding peak power limitations within the radar and by improving range resolution (larger bandwidth) [3]. These techniques are indeed combined in Space-time coded active antenna systems, where multiple codes are simultaneously transmitted through the different sub-arrays of an active antenna [4].

The availability of wideband and multiple channels opens the way to new beamforming techniques and waveforms, where different colored signals are simultaneously transmitted for coding space and time, and coherently processed in parallel on receive [5]. The available design space encompasses spatial location and sub-arrays, polarization, time, and frequency. Although time and bandwidth constraints have to be taken into account, the number of possibilities for modern MIMO radars is vast [6].

Manuscript received April 15, 2013; revised November 18, 2013; accepted January 26, 2014. Date of publication February 28, 2014; date of current version May 01, 2014.

The authors are with the Delft University of Technology, Delft, 2628CD, The Netherlands (e-mail: g.babur@tudelft.nl; p.j.aubry@tudelft.nl; f.lechevalier@tudelft.nl).

Color versions of one or more of the figures in this paper are available online at http://ieeexplore.ieee.org.

Digital Object Identifier 10.1109/TAP.2014.2309111

The principle of colored transmission, used in this study, consists in simultaneously transmitting different waveforms in the different directions, thus achieving space-time coding. This approach allows the beam-forming on transmit by means of signal processing in the MIMO radar receiver. This technique provides simultaneously wide angular coverage and angular resolution on transmit. The concept of colored space-time waveform transmission, first proposed and demonstrated by S. Drabowitch and J. Dorey [7], [8], should now be considered as sufficiently mature to be implemented on operational systems.

For practical implementation of such colored transmissions, special attention has to be given to the transmitting antenna characteristics, and especially to the mutual coupling between the antenna elements. Some recent publications investigate transmitter-induced distortions presented in the radiated signals [9], [10]. However, they are not specifically focused on the coupling on transmit. This mutual coupling indeed influences the performance in general, since in presence of mutual coupling, a specific code will then be transmitted not only through the associated antenna, but also through the other coupled antennas: obviously, the structure of the space-time coding is then partly affected by this coupling, with consequences which have to be analyzed – and hopefully mitigated.

Mutual coupling is a common problem in the applications of antenna arrays. It is a topic of continuous interest to the researchers and application engineers in the field. The coupling is present in all antenna arrays to some degree and can significantly affect their operation [11]. Investigation of the mutual coupling presented in the antenna array and development of the techniques for its compensation [e.g., 12–16 and many others]. The different effects of antenna mutual coupling on the performance of MIMO systems has been investigated [17]–[19]. However, most of the existing research on this topic does not analyze the coupling effects on transmit, which are affecting the radiated angular-dependent MIMO signal, consisting of a number of different simultaneously radiated waveforms. The coupling effects contribute to all these waveforms, corrupting the sum signal.

Notwithstanding, a MIMO radar with the space-time waveform transmission operates at a new level of complexity. It allows the transmission of the sounding signals in a wide angular angle, and, at the same time, to perform the beamforming on transmit in one (or each) of the receiving channels. It can be used for an effective monitoring of any number of beams formed on transmit by means of signal processing on receive [4], [5], [20], [21]. Therefore a deeper understanding of the antenna coupling effects on the ambiguity functions of the radiated signals is required to assess the potential performance of colored radars in actual practice. So, in this paper we consider

only the beamforming on transmit, taking into account that the beamforming on transmit and on receive are independent operations which can be considered and performed separately. In addition, the beamforming on receive can be implemented afterwards, yielding in this way the benefits from the use of both techniques.

With regard to the presented work, we assume the MIMO processor applies matched filtering to the whole transmitted signal, which is a summation in space of the orthogonal signals transmitted simultaneously through different antennas. One antenna is supposed to radiate one orthogonal signal. However, due to the mutual coupling effects, one antenna can, in principle, radiate all the signals. So, the antenna coupling effects are present to a varying degree in the compound transmitted signal and influence the beamforming performance in the receiver.

The paper analyzes the coupling effects, and proposes an adequate calibration procedure; it is organized into the following sections. Section II gives an overview of the problem due to the coupling between the transmitting array elements in the case when the colored signals are simultaneously transmitted for coding space and time. In Section III the coupling effects on the beamforming on transmit are analyzed for the ideally orthogonal signals as well as for three typical space-time codes: M-sequences, Quadratic and Cubic Alltop codes. Section IV gives a practical way to overcome the degradation due to coupling effects – a calibration technique for the beamforming on transmit, to be implemented in the radar signal processing. The coupling effects demonstration on real data and the validation of the calibration on transmit are presented in the experimental part, Section V, before the concluding Section VI.

II. Coupling Effects

Without mutual coupling between the elements, the global output s_T^0 of a linear antenna array in the angular (e.g., elevation) direction θ_0 in the absence of noise can be written as

$$s_T^0(t,\theta_0) = \sum_{n=1}^{N} P_n(\theta_0)\cdot a_n \cdot e^{j\cdot\overline{k}(\theta_0)\cdot\overline{x}(n)}\cdot s^n(t) \qquad (1)$$

where N is a number of channels on transmit; a_n is the weight amplitude applied at the nth radiating element having the embedded pattern $P_n(\theta_0)$, $\overline{k}$ is a wave-vector, and $\overline{x}\,(n)$ is the position vector of the nth radiating element. The amplitudes a_n are assumed to be equal to one and will be omitted further. The transmitted waveforms $s^n(t)$ are assumed to be orthogonal,[1] so that they can be separated from one another, on each receiving channel of a MIMO radar system. It should be emphasized that the transmitted waveforms are still bursts of periodic coded pulses, since it is a necessary condition for an efficient cancellation of long range clutter. Anyway, in this paper, we deal only with the one pulse situation, assuming that there is no Doppler effect during the duration of one pulse.

[1]Let's emphasize that the term "orthogonal" is here (and in most of the literature on MIMO radar) used in a very extended way: it actually means that the transmitted signals are orthogonal (or nearly orthogonal) for every possible relative time difference between them. This condition is necessary for the signals received from different targets or from clutter to be separated after beamforming.

Because of the linearity in Maxwell's equations, the coupling between the array elements is modeled as a linear system via the mutual coupling matrix [22]. The (N$\times$ 1) MIMO system is then simulated with the $N \times N$ coupling matrix on transmit

$$\mathbf{R}_T = \begin{bmatrix} 1 & \rho_{12} & \cdots & \rho_{1N} \\ \rho_{21} & 1 & \ddots & \rho_{2N} \\ \vdots & \ddots & \ddots & \vdots \\ \rho_{N1} & \rho_{N2} & \cdots & 1 \end{bmatrix} \qquad (2)$$

which is a complex symmetrical matrix, because for the coupling coefficients $\rho_{ij} \equiv \rho_{ji}$, and $|\rho_{1N}| < 1$. The coupling of each element with itself is considered to be equal to one – The amplitude and phase errors due to the passing of the signals through the RF part of the MIMO transmitter could be included in the main diagonal elements of $\mathbf{R}_T$.

The receive antenna is here assumed to be an individual (unspecified) antenna (this study is focused on the transmitting array).

When mutual coupling is present, the signal transmitted by the nth antenna element in the angular direction θ_0, $n \in [1 \ldots N]$, can be written as a summation

$$s_T^n(t,\theta_0) = P_n(\theta_0)\cdot \sum_{m=1}^{N} \mathbf{R}_T\,(n,m)\cdot\left(e^{j\cdot\overline{k}(\theta_0)\cdot\overline{x}(n)}\cdot s^m(t)\right) \qquad (3)$$

where m is the index of the transmitted waveform, $m \in [1 \ldots N]$.

Alternatively, due to the coupling, the mth transmitted waveform can be presented as if it were radiated by the whole antenna array

$$s_T^m(t,\theta_0) = s^m(t)\cdot \sum_{n=1}^{N} P_n(\theta_0)\cdot \mathbf{R}_T\,(n,m)\cdot e^{j\cdot\overline{k}(\theta_0)\cdot\overline{x}(n)}. \qquad (4)$$

The global signal transmitted in free space by the linear array with the presence of coupling is

$$s_T(t,\theta_0) = \sum_{n=1}^{N} s_T^n(t,\theta_0) \qquad (5)$$

or

$$s_T(t,\theta_0) = \sum_{n=1}^{N} P_n(\theta_0) \sum_{m=1}^{N} \mathbf{R}_T\,(n,m)\cdot e^{j\cdot\overline{k}(\theta_0)\cdot\overline{x}(n)}\cdot s^m(t). \qquad (6)$$

The signal (6) scattered by a point target located in the θ_0 angular direction and processed in one receiver channel r having the embedded pattern of the receiving antenna $P_r(\theta_0)$ is the following:

$$s_R^r(t,\theta_0) = P_r(\theta_0)\cdot e^{-j\cdot\overline{k}(\theta_0)\cdot\overline{x}(r)}\cdot\left(A\cdot e^{j\cdot\varphi}\right)\cdot s_T(t-\tau_0,\theta_0) \qquad (7)$$

where A and φ are the amplitude and phase of the complex scattering coefficient of an observed target, $\dot{A} = A\cdot e^{j\cdot\varphi}$, τ_0 is a time delay defined by the travelling distance of the signal. We assume that within one sounding pulse the effects of the observed object motion (Doppler) don't show up. Otherwise the Doppler frequency shift should be added in (7).

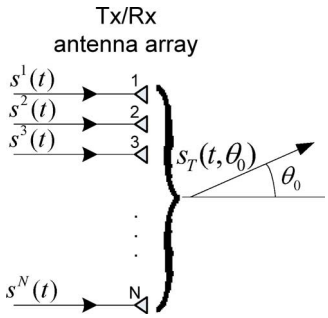

Fig. 1. MIMO transmission.

The beamforming on transmit is performed (on the received signals) by the pulse compression filter, matched with the ideal transmitted signals [see (1)]

$$R^r_{\theta_0}(\tau,\theta') = \int s^0_T(t-\tau,\theta')\cdot(s^r_R(t,\theta_0))^* dt \tag{8}$$

where θ_0 is the implicit position of the target and the superscript '$*$' means complex conjugation.

Equation (8) in the extended form can be written as

$$R^r_{\theta_0}(\tau,\theta') = P_r(\theta_0)\cdot\dot{A}^*\cdot e^{+j\cdot\overline{k}(\theta_0)\cdot\overline{x}(r)} \cdot\int s^0_T(t-\tau,\theta')\cdot(s_T(t-\tau_0,\theta_0))^* dt \tag{9}$$

where θ' is a hypothesis about the direction of arrival, which covers the angular domain $[\theta_{\min}\ldots\theta_{\max}]$.

Ambiguity function analysis implies taking the absolute value from the matched filter output. So, we can omit the constant phase term $e^{-j\cdot\overline{k}(\theta_0)\cdot\overline{x}(r)}$ characteristic for the rth receiving channel. Since our study is focused on the transmitting array, and the calibration of antenna arrays on transmit and on receive are two separate procedures, which, in principle, are independent, we can also omit the pattern of the receiving element $P_r(\theta_0)$ as long as it remains the same for all the components within $s_T(t-\tau_0,\theta_0)$ in (7). Changing also the time variables $t'=(t-\tau_0)$, $\tau'=(\tau_0-\tau)$, we receive

$$R_{\theta_0}(\tau',\theta') = \int s^0_T(t'+\tau',\theta')\cdot(s_T(t',\theta_0))^* dt' \tag{10}$$

and in the extended form

$$R_{\theta_0}(\tau',\theta') = \int\left(\sum_{n'=1}^{N} e^{j\cdot\overline{k}(\theta')\cdot\overline{x}(n')}\cdot s^{n'}(t'+\tau')\right) \cdot\left(\sum_{n=1}^{N} P_n(\theta_0)\sum_{m=1}^{N}\mathbf{R}_T(n,m)\cdot e^{j\cdot\overline{k}(\theta_0)\cdot\overline{x}(n)}\cdot s^m(t')\right)^* dt' \tag{11}$$

where, as we remember, the indexes n and n' denote the antenna elements on transmit (for the transmitted signal and for its replica, respectively), while m is the index number for the orthogonal transmitted signals. The replica of the radiated signals does not contain the antenna patterns. The replicas of the generated signals are recorded in the radar transmitter. In turn, the phase term containing the wave-vector and the position vector are added by means of the signal processing.

Considering the fact that $\mathbf{R}_T(n,m)=1$ if $n=m$, (6) can be represented as

$$s_T(t) = s^0_T(t) + s^{er}_T(t) \tag{12}$$

where

$$s^{er}_T(t) = \sum_{n=1}^{N} P_n(\theta_0)\sum_{m\neq n}^{N}\mathbf{R}_T(n,m)\cdot e^{j\cdot\overline{k}(\theta_0)\cdot\overline{x}(n)}\cdot s^m(t).$$

Respectively, (11) can split into two parts

$$R_{\theta_0}(\tau',\theta') = R^0_{\theta_0}(\tau',\theta') + R^{er}_{\theta_0}(\tau',\theta') \tag{13}$$

where $R^0_{\theta_0}(\tau',\theta')$ is the ideal compressed signal without coupling between antenna elements

$$R^0_{\theta_0}(\tau',\theta') = N\cdot\sum_{n=1}^{N} P_n(\theta_0)\cdot\sum_{n'=1}^{N} e^{j\cdot\left(\overline{k}(\theta')\cdot\overline{x}(n)-\overline{k}(\theta_0)\cdot\overline{x}(n')\right)} \cdot\int s^n(t'+\tau')\cdot\left(s^{n'}(t')\right)^* dt'. \tag{14}$$

The mathematical expression of the multiparameter signal $R^0_{\theta_0}(\tau',\theta')$ shows its dependency on the transmitted waveforms $s^n(t)$, which, in principle, should be mutually orthogonal. The ambiguity function $\left|R^0_{\theta_0}(\tau',\theta')\right|^2$ is thus a 3-D function, giving for each aiming direction θ_0 the delay-angle ambiguity. $R^0_{\theta_0}(\tau',\theta')$ being a 3-parameters function, it cannot be visualized easily: a preferred way is to look at the angle-angle cut, for $\tau=0$, and at the range-angle ambiguity, for a specific θ_0:

- $\left|R^0_{\theta_0}(0,\ \sin\theta)\right|^2 = D^0(\theta,\theta_0)$, is the angular transmit diagram (at the exact range of the target, $\tau'=\tau_0$), as a function of the angular aiming position θ_0 .
- $\left|R^0_{\theta_0}\left((c\cdot\tau')/2,\theta'\right)\right|^2$, where θ_0 is constant, is the range-angle ambiguity function, for the considered aiming direction – Ideally, this range angle ambiguity function should also be analyzed for each possible aiming direction θ_0.

Figs. 2–4 present these cuts of $R^0_{\theta_0}(\tau',\theta')$ and demonstrate, as examples, the potential of implementation of three different waveform types: M-sequences, quadratic Alltop sequences and cubic Alltop sequences with BT-product 255 which was chosen relatively small for better visibility of the presented figures. The angle-angle cut for $\tau'=\tau_0$, that is $\tau'=0$, and the range-angle cut for $\theta_0=0$ are presented for the case $N=8$.

For analysis of the coupling effects for space-time radar waveforms, we should analyze the error signal, which for the implicit aiming direction θ_0 can be derived from (11) and (14) as

$$R^{er}_{\theta_0}(\tau',\theta') = \int\left(\sum_{n'=1}^{N} e^{j\cdot\overline{k}(\theta')\cdot\overline{x}(n')}\cdot s^{n'}(t'+\tau')\right) \cdot\left(\sum_{n=1}^{N} P_n(\theta_0)\sum_{m\neq n}^{N}\mathbf{R}_T(n,m)\cdot e^{j\cdot\overline{k}(\theta_0)\cdot\overline{x}(n)}\cdot s^m(t')\right)^* dt' \tag{15}$$

$$R^{er}_{\theta_0}(\tau',\theta') = \sum_{n=1}^{N} P_n(\theta_0)\sum_{n'=1}^{N}\sum_{m\neq n'}^{N} e^{j\cdot\left(\overline{k}(\theta')\cdot\overline{x}(n')-\overline{k}(\theta_0)\cdot\overline{x}(n)\right)} \cdot\mathbf{R}^*_T(n,m)\cdot\int s^{n'}(t'+\tau')\cdot(s^m(t'))^* dt'. \tag{16}$$

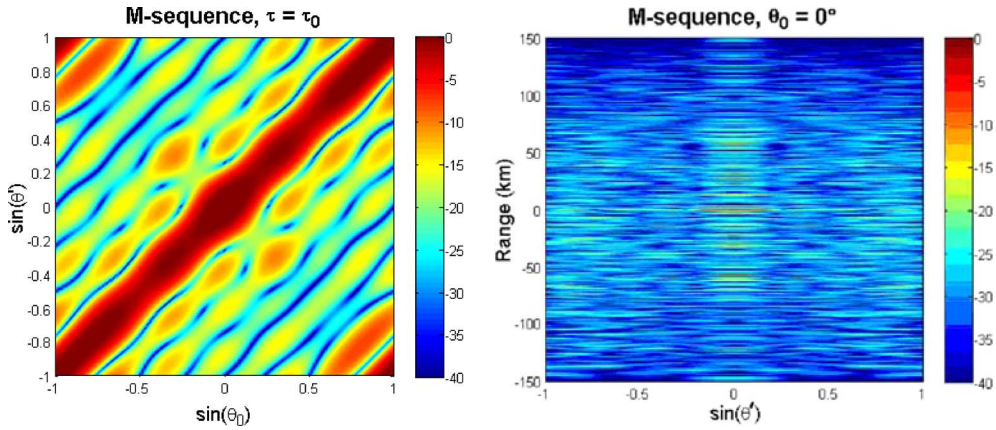

Fig. 2. M-sequences: angle-angle and range-angle cut (in dB, normalized) of the ambiguity function, no coupling.

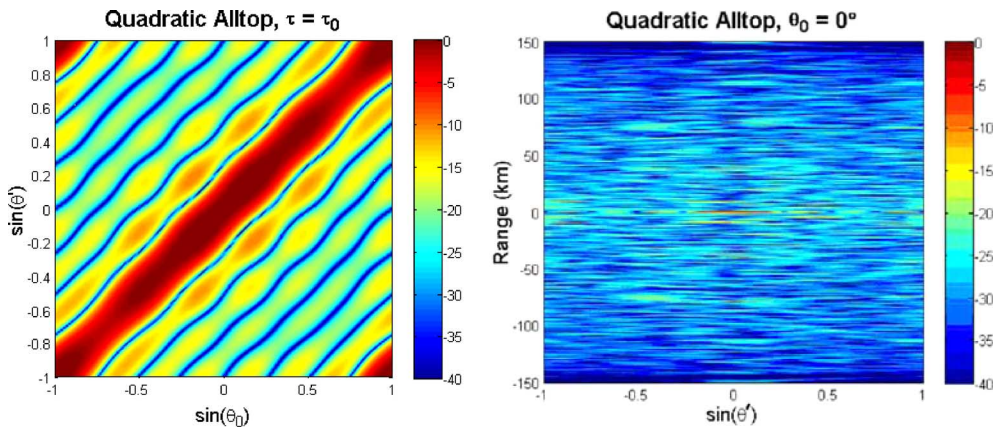

Fig. 3. Eight quadratic Alltop sequences: angle-angle and range-angle cut (in dB, normalized) of the ambiguity function, no coupling.

Taking into account that the normalized self-coupling ($m = n'$) integral between the orthogonal waveforms is equal to *1* and the normalized cross-coupling integral ($m \neq n'$) in case of (almost) orthogonal waveforms with large BT-products is equal to *0* for $\tau' = 0$ [23], that is $\tau = \tau_0$, (16) can be simplified:

$$R^{er}_{\theta_0,\tau_0}(\theta') = N \cdot \sum_{n=1}^{N} P_n(\theta_0) \sum_{n' \neq n}^{N} e^{j\cdot\left(\overline{k}(\theta')\cdot\overline{x}(n') - \overline{k}(\theta_0)\cdot\overline{x}(n)\right)} \cdot \mathbf{R}^*_T(n,n'). \tag{17}$$

As previously stated, the radar waveforms $s^n(t)$ occupying the same time interval and the same bandwidth can not be completely orthogonal, that is (17) is an approximation of the error signal for the case of the ideally orthogonal waveforms. Different examples with ideal waveforms as well as with real waveforms are given in the following.

III. Coupling Effects Analysis

To analyze the coupling effect on $R^{er}_{\theta_0}(\tau', \theta')$, the coupling matrix (2) should be specified. Initially we assume that the coupling between the adjacent elements is equal to ρ and 0 between the farther elements of the array. The coupling matrix on transmit becomes

$$\mathbf{R}_T = \begin{bmatrix} 1 & \rho & 0 & \dots & 0 \\ \rho & 1 & \rho & \ddots & \vdots \\ 0 & \rho & 1 & \rho & 0 \\ \vdots & \ddots & \rho & 1 & \rho \\ 0 & \dots & 0 & \rho & 1 \end{bmatrix}. \tag{18}$$

Then the error signal (17) can be rewritten as follows:

$$R^{er}_{\theta_0,\tau_0}(\theta') = N \cdot \rho \cdot \left(\sum_{n=2}^{N} P_n(\theta_0) \sum_{n'=(n-1)} e^{j\cdot\left(\overline{k}(\theta')\cdot\overline{x}(n) - \overline{k}(\theta_0)\cdot\overline{x}(n')\right)} + \sum_{n=1}^{(N-1)} P_n(\theta_0) \sum_{n'=(n+1)} e^{j\cdot\left(\overline{k}(\theta')\cdot\overline{x}(n) - \overline{k}(\theta_0)\cdot\overline{x}(n')\right)} \right). \tag{19}$$

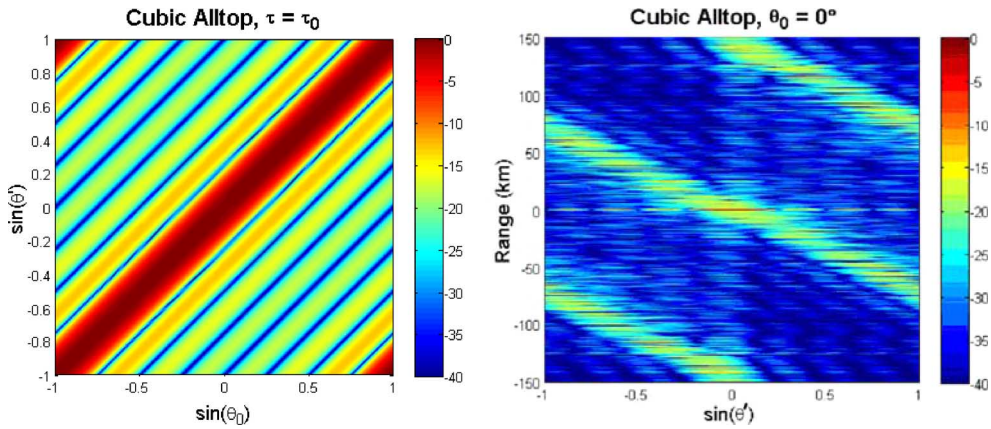

Fig. 4. Eight cubic Alltop sequences: angle-angle and range-angle cut (in dB, normalized) of the ambiguity function, no coupling.

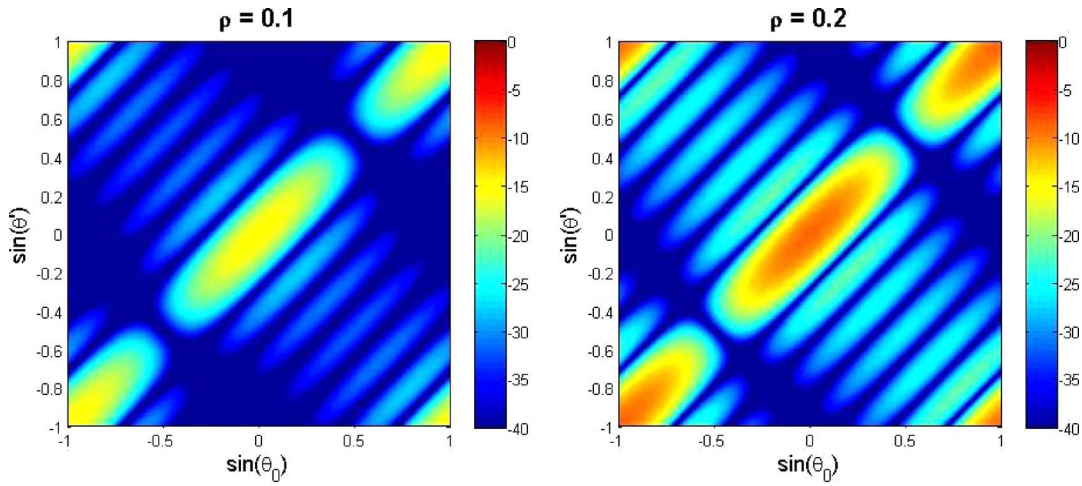

Fig. 5. Angle-angle error signal in case of the ideally orthogonal waveforms (in dB, normalized) and the simplified coupling matrix approximation for (a) $\rho = 0.1$ and (b) $\rho = 0.2$. (a) $\mathrm{Max} = -15.1$ dB. (b) $\mathrm{Max} = -9.1$ dB.

Then we represent the position vector of the $(n+1)$th radiating element with respect to the position of the nth element as $\overline{x}\,(n)+\Delta x$, and for the $(n-1)$th radiating element as $\overline{x}\,(n)-\Delta x$, where Δx is the distance between two adjacent elements of the uniform linear array. The error signal becomes

$$R^{er}_{\theta_0,\tau_0}(\theta') = N\cdot\rho\cdot\left(e^{j\cdot\left(\overline{k}(\theta_0)\cdot\Delta x\right)}\cdot\sum_{n=2}^{N}P_n(\theta_0)\cdot e^{j\cdot\overline{x}(n)\cdot\left(\overline{k}(\theta')-\overline{k}(\theta_0)\right)} + e^{-j\cdot\left(\overline{k}(\theta_0)\cdot\Delta x\right)}\cdot\sum_{n=1}^{(N-1)}P_n(\theta_0)\cdot e^{j\cdot\overline{x}(n)\cdot\left(\overline{k}(\theta')-\overline{k}(\theta_0)\right)}\right) \tag{20}$$

and for considered example can be presented as a three terms summation. The first term describes the main contribution of the coupling in the compressed signal for the considered example. The second and the third terms complete the equation and correspond to the edge, *1* and N, antenna elements

$$R^{er}_{\theta_0,\tau_0}(\theta') = N\cdot\rho\cdot \cdot\left(\begin{array}{l} 2\cdot\cos\left(\overline{k}(\theta_0)\cdot\Delta x\right)\cdot\sum_{n=2}^{N-1}P_n(\theta_0)\cdot e^{j\cdot\overline{x}(n)\cdot\left(\overline{k}(\theta')-\overline{k}(\theta_0)\right)} \\ \quad +e^{j\cdot\left(\overline{k}(\theta_0)\cdot\Delta x\right)}\cdot P_N(\theta_0)\cdot e^{j\cdot\overline{x}(N)\cdot\left(\overline{k}(\theta')-\overline{k}(\theta_0)\right)} \\ \quad +e^{-j\cdot\left(\overline{k}(\theta_0)\cdot\Delta x\right)}\cdot P_1(\theta_0)\cdot e^{j\cdot\overline{x}(1)\cdot\left(\overline{k}(\theta')-\overline{k}(\theta_0)\right)} \end{array}\right). \tag{21}$$

Based on the first term of the sum (21), the following conclusions can be made for the approximation (18):

- the error signal is proportional to the parameter ρ;
- the factor $\cos\left(\overline{k}(\theta_0)\cdot\Delta x\right)$ results in the amplitude deviation along the line $\theta' = \theta_0$;
- the factor $\cos\left(\overline{k}(\theta_0)\cdot\Delta x\right)$ is maximal for $\theta_0 = 0$. So, the maximal error value is expected in the $\theta_0 = 0$ direction.

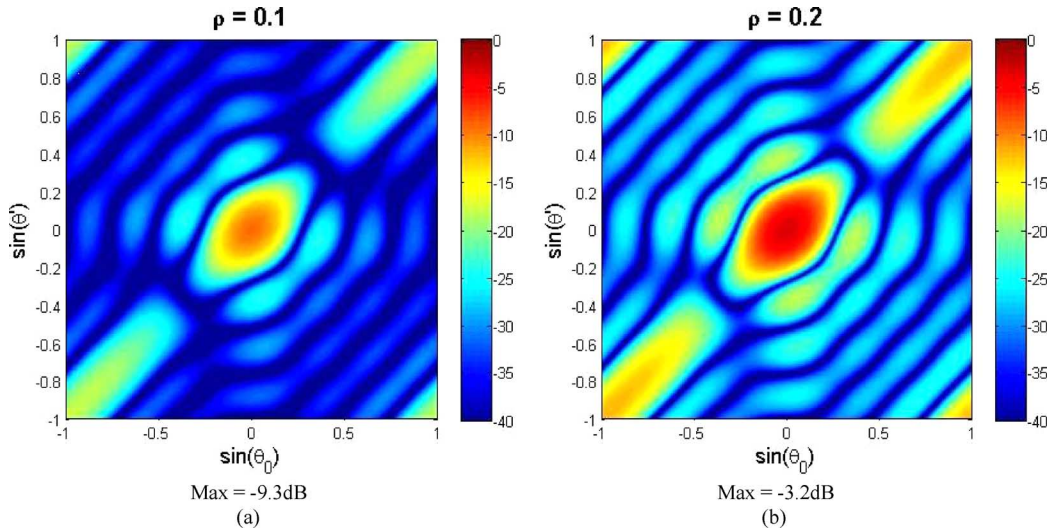

Fig. 6. Angle-angle error signal in case of the ideally orthogonal waveforms (in dB, normalized) and the full coupling matrix approximation for (a) $\rho = 0.1$ and (b) $\rho = 0.2$. (a) $\mathrm{Max} = -9.3$ dB. (b) $\mathrm{Max} = -3.2$ dB.

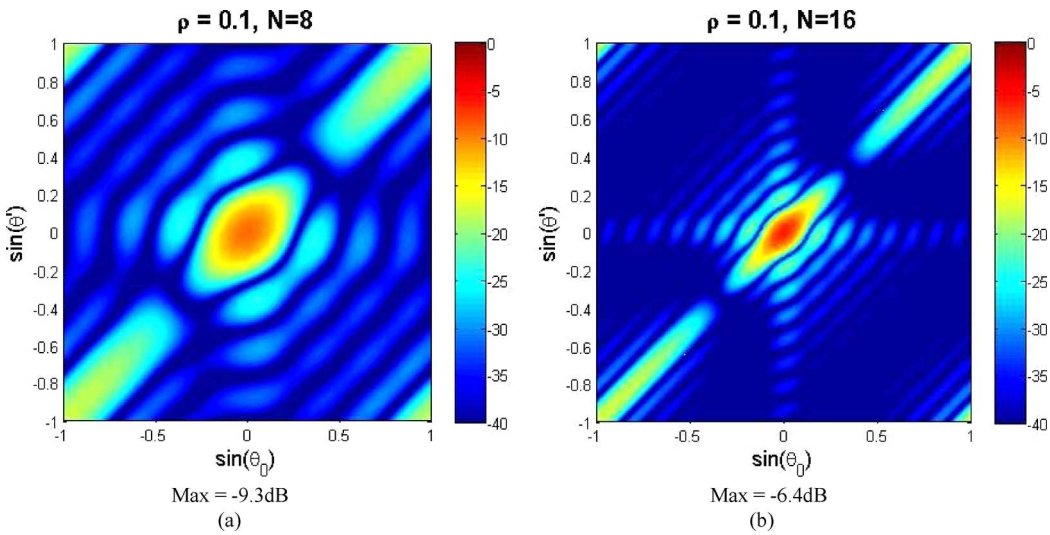

Fig. 7. Angle-angle error signal in case of the ideally orthogonal waveforms (in dB, normalized) for (a) $N = 8$ and (b) $N = 16$. (a) $\mathrm{Max} = -9.3$ dB. (b)$\mathrm{Max} = -6.4$ dB.

- the phase of the coupling coefficient does not influence the amplitude of the error value because ρ is a common factor in (21).

For large linear arrays when $N \gg 1$ the contribution of the edge elements can be omitted and

$$R^{er}_{\theta_0,\tau_0}(\theta') \approx 2 \cdot N \cdot \rho \cdot \cos\left(\overline{k}(\theta_0) \cdot \Delta x\right) \cdot \cdot \sum_{n=2}^{N-1} P_n(\theta_0) \cdot e^{j \cdot \overline{x}(n) \cdot \left(\overline{k}(\theta') - \overline{k}(\theta_0)\right)} = = 2 \cdot N \cdot \rho \cdot \cos\left(\overline{k}(\theta_0) \cdot \Delta x\right) \cdot D^{er}(\theta_0, \theta') \quad (22)$$

where due to the coupling effects the error is proportional to the diagram $D^{er}(\theta_0, \theta') = \sum_{n=2}^{N-1} P_n(\theta_0) \cdot e^{j \cdot \overline{x}(n) \cdot \left(\overline{k}(\theta') - \overline{k}(\theta_0)\right)}$ created with the shortened aperture by $[2, \ldots, N-1]$ elements. In case of a regular array, with $\lambda/2$ spacing between elements, the error is proportional to $\cos(\pi \sin \theta_0)$, maximal for $\theta_0 = 0$, and null for $\theta_0 = \pi/3$.

The coupling matrix (18) has been modeled and the error signal for different values of ρ has been calculated. Fig. 5 presents the error signal $\left|R^{er}_{\theta_0}(\tau', \theta')\right|^2$ normalized with regard to the maximal value of the useful signal for the case $N = 8$. The waveforms $s^n(t)$ have been assumed to be ideally orthogonal. The error signal for each specific direction θ_0 presents the parasitic pattern superimposed on the beam formed due to the colored space-time waveform transmission. Obviously, the error is larger with a stronger coupling between the array elements. We see also that the value of the error signal doesn't change with the phase change of the coupling parameter for the considered example.

As we see from (2), the coupling in antenna arrays is not limited to the coupling between the adjacent elements, but it weakens with increasing distance between the corresponding elements. It is possible to exploit certain properties of the coupling for reducing the computational complexity of (2) [24]. One such property is the inverse dependence of coupling coefficients on

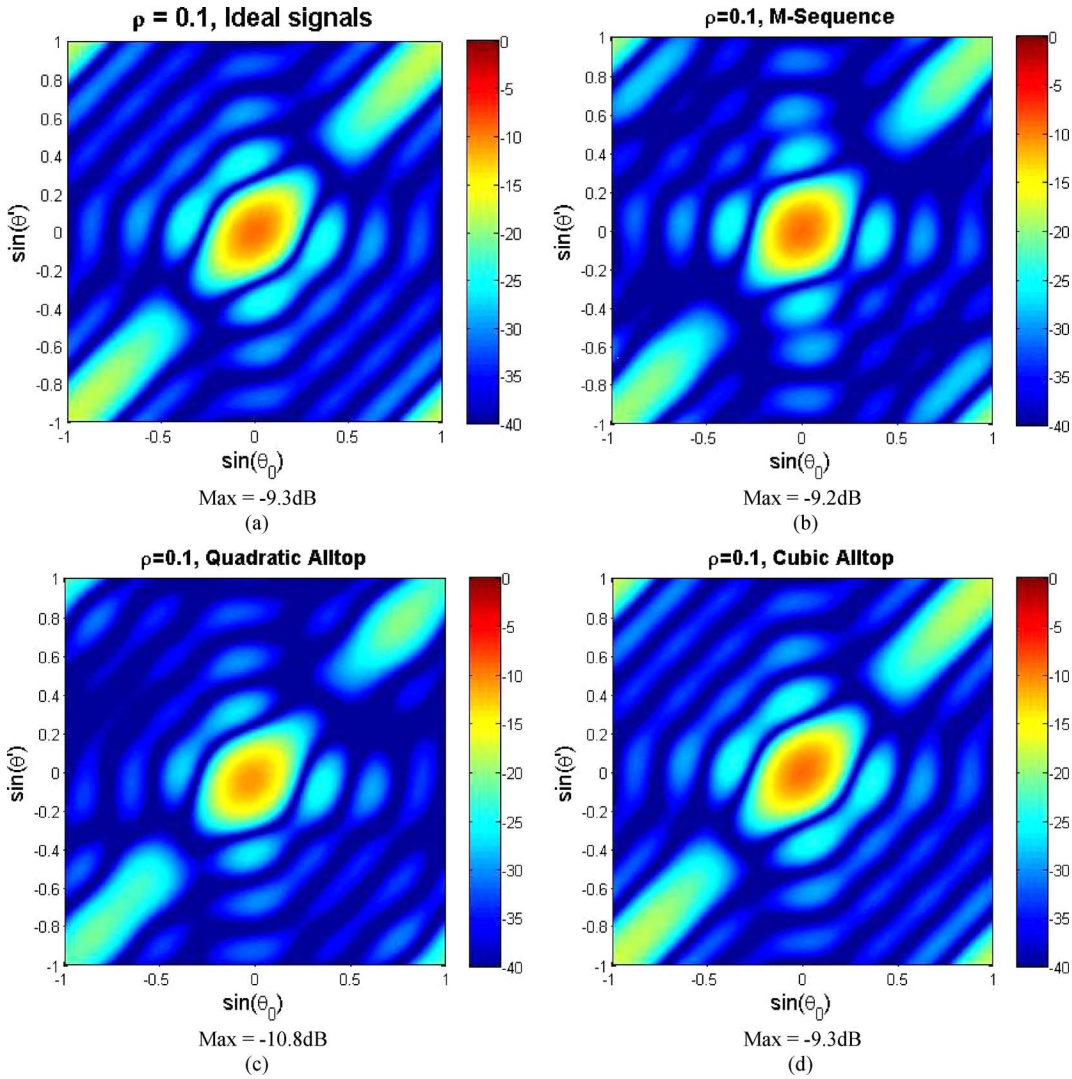

Fig. 8. Angle-angle error signal (in dB, normalized) for (a) ideally orthogonal signals, (b) M-sequences, (c) quadratic, and (d) cubic Alltop sequences, $\rho = 0.1$. (a) $\mathrm{Max} = -9.3$ dB. (b) $\mathrm{Max} = -9.2$ dB. (c) $\mathrm{Max} = -10.8$ dB. (d) $\mathrm{Max} = -9.3$ dB.

the distance between the array elements [25]. Using this property in combination with the parameter ρ (the coupling between the adjacent elements), the full coupling matrix can be approximated as follows:

$$\mathbf{R}_T = \begin{bmatrix} 1 & \rho & \frac{\rho}{2} & \cdots & \frac{\rho}{(N-1)} \\ \rho & 1 & \rho & \ddots & \vdots \\ \frac{\rho}{2} & \rho & 1 & \rho & \frac{\rho}{2} \\ \vdots & \ddots & \rho & 1 & \rho \\ \frac{\rho}{(N-1)} & \cdots & \frac{\rho}{2} & \rho & 1 \end{bmatrix}. \qquad (23)$$

The approximation 23 can represent the worst case, when the phases of the coupling coefficients between the elements remain the same and contribute to the error signal in phase.

The modeling results for the error signal in the case of such a full coupling matrix, when all antenna elements contribute to the errors on the beamforming on transmit and the amplitude of the coupling decays rather slow with the distance increase, are presented in Fig. 6. The normalized error signal have been calculated for the coupling parameter $\rho = \{0.1, 0.2\}$ and $N = 8$, the waveforms are still considered as ideally orthogonal. The comparison of Figs. 5 and 6 shows that relatively strong influence of other elements, not only adjacent, increases the error value and focuses more the error signal around the zero angular direction. . When the coupling is relatively large (for example, Fig. 6(b)), the error value (-3.2 dB) becomes comparable with the useful signal (the normalized maximum of the ambiguity function is equal to 0 dB).

In case of the array size change, the maximal value and general behavior of the error signals remain the same. The change of the error signal $\left|R^{er}_{\theta_0}(\tau', \theta')\right|^2$ for the specific beam-formed directions θ_0 (narrowing for a bigger N) is defined by the parasitic antenna pattern due to the coupling, which was introduced in the previous paragraph, see Fig. 7.

Figs. 5–7 demonstrate the global effect of the coupling on the beamforming for the colored waveform transmission. However, real signals having overlapping bandwidths and occupying the same time interval can not be completely orthogonal for all relative time delays. The angle-angle error for different types of sounding signals is shown in Fig. 8. The presented results

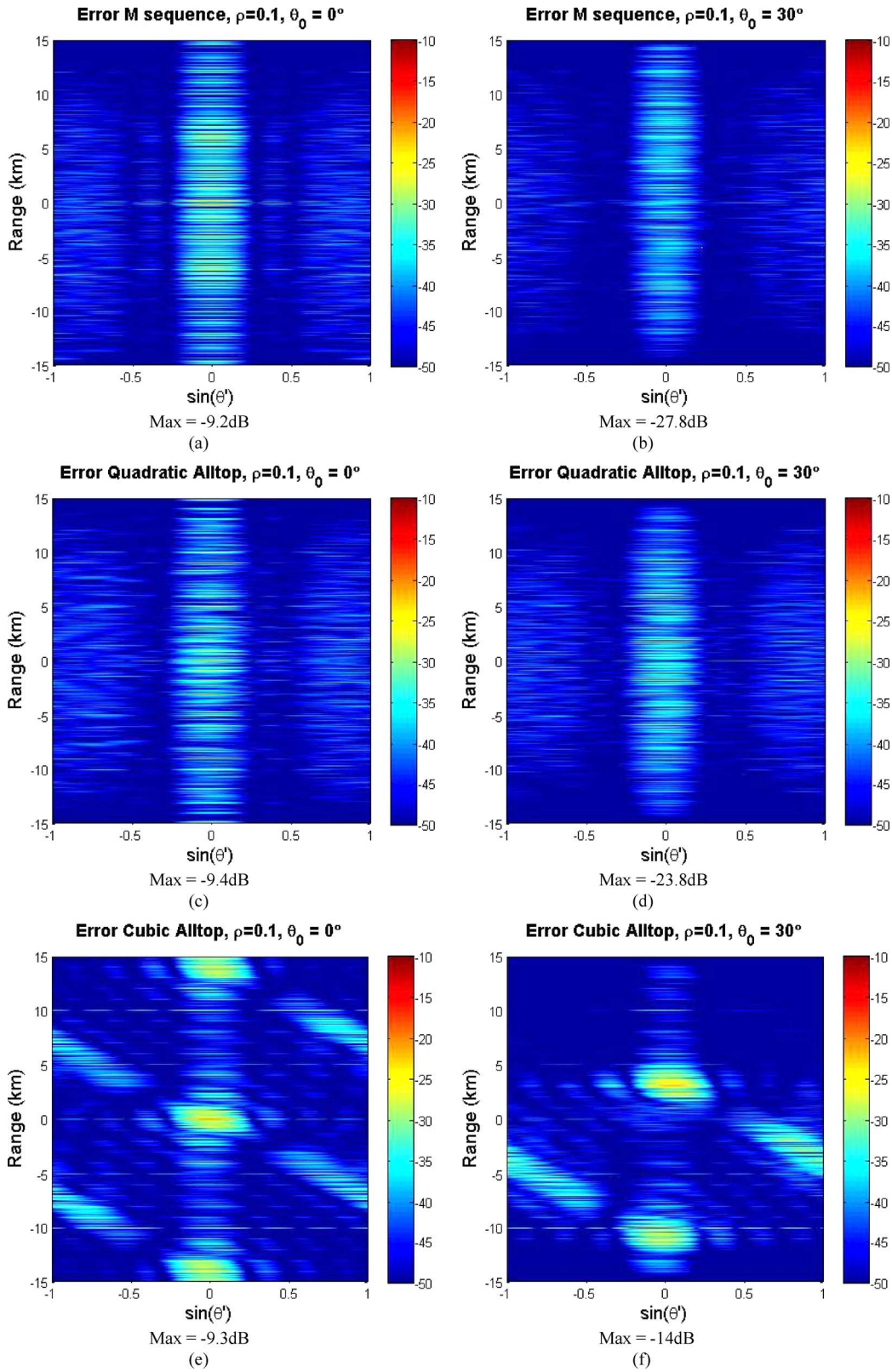

Fig. 9. Angle-range error signal (in dB, normalized) for different waveforms for the aiming directions . $\theta_0 = \{0°, 30°\}$. (a) $\mathrm{Max} = -9.2$ dB. (b) $\mathrm{Max} = -27.8$ dB. (c) $\mathrm{Max} = -9.4$ dB. (d) $\mathrm{Max} = -23.8$ dB. (e) $\mathrm{Max} = -9.3$ dB. (f) $\mathrm{Max} = -14$ dB.

demonstrate a good agreement between the idealization of the signals' orthogonality [Fig. 8(a)] and the real signals' contribution [Fig. 8(b)–(d)]. Normally the waveforms with larger BT-products provide higher orthogonality with regard to each other, and, therefore greater proximity to the ideally orthogonal signals.

For the considered example M-sequences demonstrate the widening effect and higher error for the main beam in $\theta_0 =$

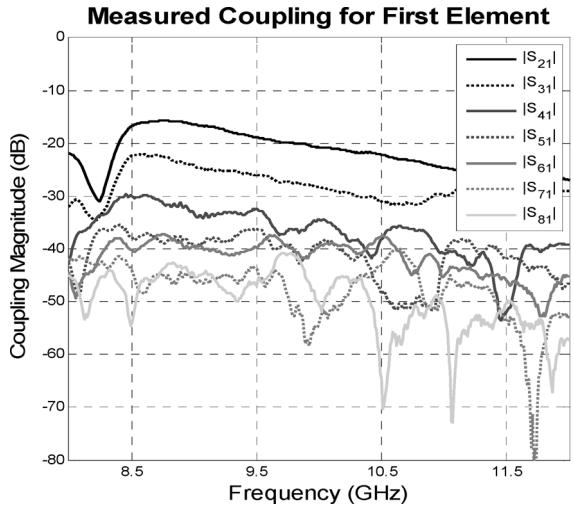

Fig. 10. Coupling measurements.

$0°$ direction. Conversely, the cubic Alltop sequences provide an error signal equivalent to the ideally orthogonal signals. The sidelobes in the error signal for the real signals, Fig. 8(b)–(d), remain at the same level as for the ideally orthogonal signals.

Since the multiparameter signal $R_{\theta_0}(\tau',\theta')$ is affected by the coupling influence, it would be interesting to look at the range-angle cuts along some implicit positions θ_0 of the target. The ideally orthogonal waveforms are not of interest here, because they do not give rise to any sidelobes in range.

Fig. 9 shows the range-angle cut of the error signal $\left|R^{er}_{\theta_0}(\tau',\theta')\right|^2$ (in dB) at $\tau = 0$ for $\theta_0 = 0°$ and $\theta_0 = 30°$ for $\rho = 0.1$ in case of space-time coding for the same codes considered before: M-sequences, quadratic Alltop and cubic Alltop sequences. For all the considered signals the influence of the array factor is visible along the angular direction at all ranges. At the same time, the sidelobes for cubic Alltop signals form the inclined edge corresponding to a coupling between range and angle. The error value is rather large for $\theta_0 = 0°$ and comparable with the sidelobe level of the ambiguity functions, see Figs. 2–4. It means that the error due to a strong target can mask the signal from a weal target and, therefore the calibration on transmit is desired for mitigating this error. The error signal at $\theta_0 = 30°$ is much lower than the sidelobe level of the ambiguity functions, and the error influence might be neglected.

IV. Calibration Technique

The idea of calibration technique on transmit is based on the fact that the coupling effects presented in the radiated group signal (6) can be compensated, if amplitudes of the transmitted signals' replica used for matched filtering in one receiving channel are changed appropriately. So, the modified replica of the transmitted signal (1) for compensation of the coupling effect can be presented as

$$s^0_T(t,\theta_0) = \sum_{n=1}^{N} P_n(\theta_0)\cdot(a_n + A^c_n)\cdot e^{j\cdot\overline{k}(\theta_0)\cdot\overline{x}(n)}\cdot s^n(t) \tag{24}$$

where A^c_n are the complex amplitudes of the correcting signals. Normally, the amplitudes a_n are considered as equal to one. So, the correcting signal imposed on the transmitted signal replica in a receiver channel for the coupling effect calibration can be written as:

$$s^c_T(t,\theta_0) = \sum_{n=1}^{N} P_n(\theta_0)\cdot A^c_n\cdot e^{j\cdot\overline{k}(\theta_0)\cdot\overline{x}(n)}\cdot s^n(t). \tag{25}$$

With correction of the coupling effects, the compressed signal (13) splits into three components

$$R_{\theta_0}(\tau',\theta') = R^0_{\theta_0}(\tau',\theta') + R^{er}_{\theta_0}(\tau',\theta') + R^c_{\theta_0}(\tau',\theta') \tag{26}$$

where the first component $R^0_{\theta_0}(\tau',\theta')$ is the signal without the coupling influence, and third component $R^c_{\theta_0}(\tau',\theta')$ should compensate the second, error component:

$$R^c_{\theta_0}(\tau',\theta') = -R^{er}_{\theta_0}(\tau',\theta'). \tag{27}$$

The example in the previous Section has shown that the error signal due to the coupling effects is approximated pretty well with the coupling between the adjacent antenna elements (see (19), without taking into account the full coupling matrix (see (2) and (18)). However, for calibration of real arrays we should take into account real (measured) coupling $\rho_{i,j}$ between the adjacent array elements, $|i-j| = 1$, $i,j \in [1\ldots N]$. Thus, the following approximation of the coupling matrix is used for the calibration; the correcting signals are applied on the useful signals corresponding to the main diagonal:

$$\mathbf{R}_T = \begin{bmatrix} (1-A^c_1) & \rho_{12} & 0 & \ldots & 0 \\ \rho_{21} & (1-A^c_2) & \rho_{23} & \ddots & \vdots \\ 0 & \rho_{32} & (1-A^c_3) & \ddots & 0 \\ \vdots & \ddots & \ddots & \ddots & \rho_{(N-1)N} \\ 0 & \ldots & 0 & \rho_{N(N-1)} & (1-A^c_N) \end{bmatrix}. \tag{28}$$

According to (28), the error signal, which was written as (17) in the case for the ideally orthogonal signals, becomes

$$\begin{aligned} &R^{er}_{\theta_0,\tau_0}(\theta') \\ &= N\cdot\Bigg[e^{j\cdot\left(\overline{k}(\theta_0)\cdot\Delta x\right)}\sum_{n=2}^{N} P_n(\theta_0)\cdot\rho_{n(n-1)}\cdot e^{j\cdot\overline{x}(n)\left(\overline{k}(\theta')\cdot-\overline{k}(\theta_0)\right)} \\ &\quad + e^{-j\cdot\left(\overline{k}(\theta_0)\cdot\Delta x\right)}\sum_{n=1}^{N-1} P_n(\theta_0)\cdot\rho_{n(n+1)}\cdot e^{j\cdot\overline{x}(n)\left(\overline{k}(\theta')\cdot-\overline{k}(\theta_0)\right)}\Bigg] \end{aligned} \tag{29}$$

or

$$\begin{aligned} &R^{er}_{\theta_0,\tau_0}(\theta') \\ &= N\cdot\Bigg[\sum_{n=2}^{N-1} P_n(\theta_0)\cdot\Big(\rho_{n(n-1)}\cdot e^{j\cdot\left(\overline{k}(\theta_0)\cdot\Delta x\right)} \\ &\quad +\rho_{n(n+1)}e^{-j\cdot\left(\overline{k}(\theta_0)\cdot\Delta x\right)}\Big)\cdot e^{j\cdot\overline{x}(n)\left(\overline{k}(\theta')\cdot-\overline{k}(\theta_0)\right)} \\ &\quad + P_1(\theta_0)\cdot\rho_{12}\cdot e^{-j\cdot\left(\overline{k}(\theta_0)\cdot\Delta x\right)}\cdot e^{j\cdot\overline{x}(1)\left(\overline{k}(\theta')\cdot-\overline{k}(\theta_0)\right)} \\ &\quad + P_N(\theta_0)\cdot\rho_{N(N-1)}\cdot e^{j\cdot\left(\overline{k}(\theta_0)\cdot\Delta x\right)}\cdot e^{j\cdot\overline{x}(N)\left(\overline{k}(\theta')\cdot-\overline{k}(\theta_0)\right)}\Bigg]. \end{aligned} \tag{30}$$

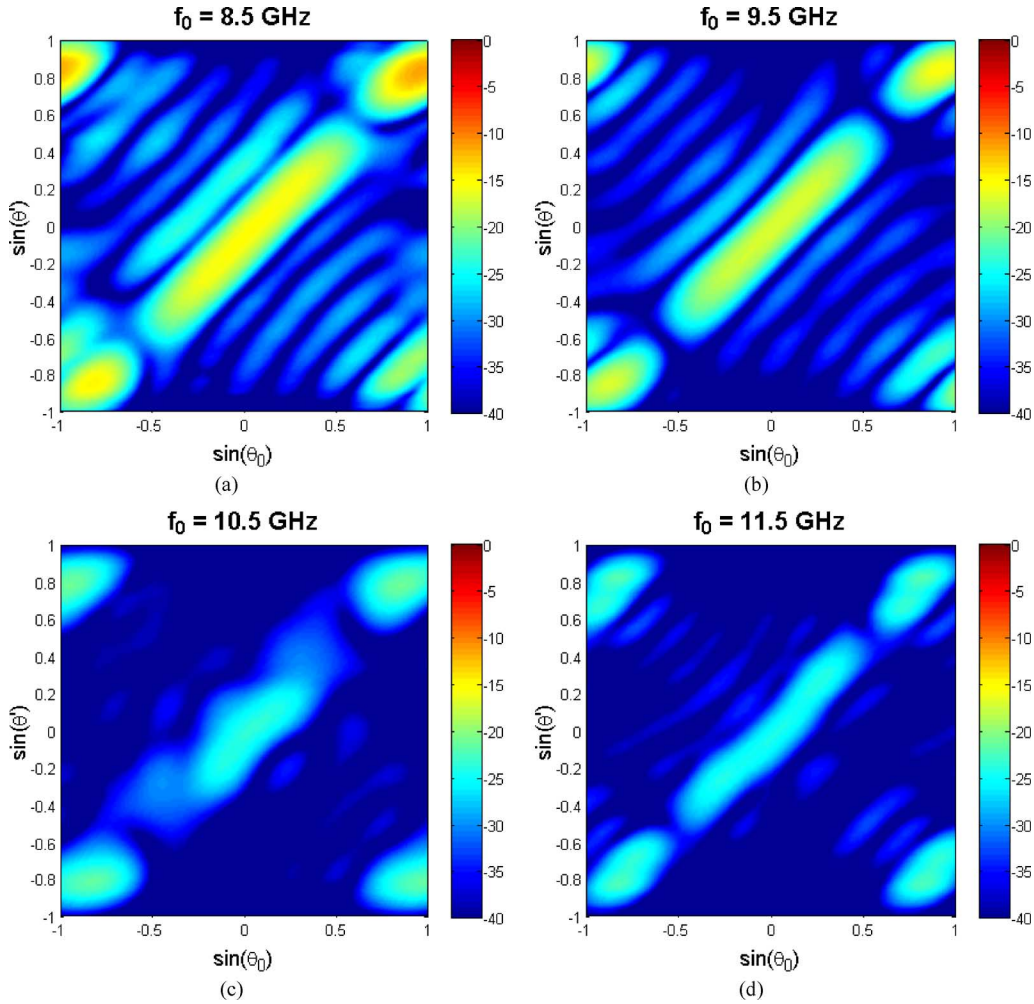

Fig. 11. Angle-angle error $\left|R^{cr}_{\theta_0}(\tau'=0,\theta')\right|^2$ for eight ideally orthogonal signals for the real antenna coupling and for real patterns of the array elements at (a) 8.5 GHz; (b) 9.5 GHz; (c) 10.5 GHz; (d) 11.5 GHz.

From whence the amplitudes of the correcting signal amplitudes are derived as

$$A^c_{n,\theta_0} = \begin{cases} -\rho_{12}\cdot P_2(\theta_0)\cdot e^{-j\cdot\left(\overline{k}(\theta_0)\cdot\Delta x\right)}, n=1; \\ -\begin{pmatrix} \rho_{n(n-1)}\cdot P_{n-1}(\theta_0)\cdot e^{j\cdot\left(\overline{k}(\theta_0)\cdot\Delta x\right)} \\ +\rho_{n(n+1)}\cdot P_{n+1}(\theta_0)\cdot e^{-j\cdot\left(\overline{k}(\theta_0)\cdot\Delta x\right)} \end{pmatrix}, \\ n=2,\ldots,N-1; \\ -\rho_{N(N-1)}\cdot P_{N-1}(\theta_0)\cdot e^{j\cdot\left(\overline{k}(\theta_0)\cdot\Delta x\right)}, n=(N-1). \end{cases} \quad (31)$$

The obtained equation takes into account the coupling between the radiating elements of the array, as well as . the radiation pattern of each antenna element, $P_n(\theta_0)$. Equation (31) shows that due to the coupling the nth waveform is radiated with the coefficient $\rho_{n(n-1)}$ via the $(n-1)$th element and with the coefficient $\rho_{n(n+1)}$ via the $(n+1)$th element, which have the radiated patterns $P_{n-1}(\theta_0)$ and $P_{n+1}(\theta_0)$, correspondingly.

The coupling effects and, therefore, the calibration technique described by the coefficients in (31) are not range dependent. Hence, the developed calibration technique is supposed to be efficient for observation of point, as well as distributed radar objects.

V. Experiment

The coupling between the eight elements of a suitable X-band antenna array was measured using a vector network analyzer. The antenna is an array of 32 by 4 X-band patches. The radiation patterns and the coupling of 8 elements have been measured in the operating configuration. In this way, the measured patterns are taking into account the coupling effects. The selected line of 8 elements is performing as a linear equidistant array. The remaining elements are terminated by 50 Ω loads,

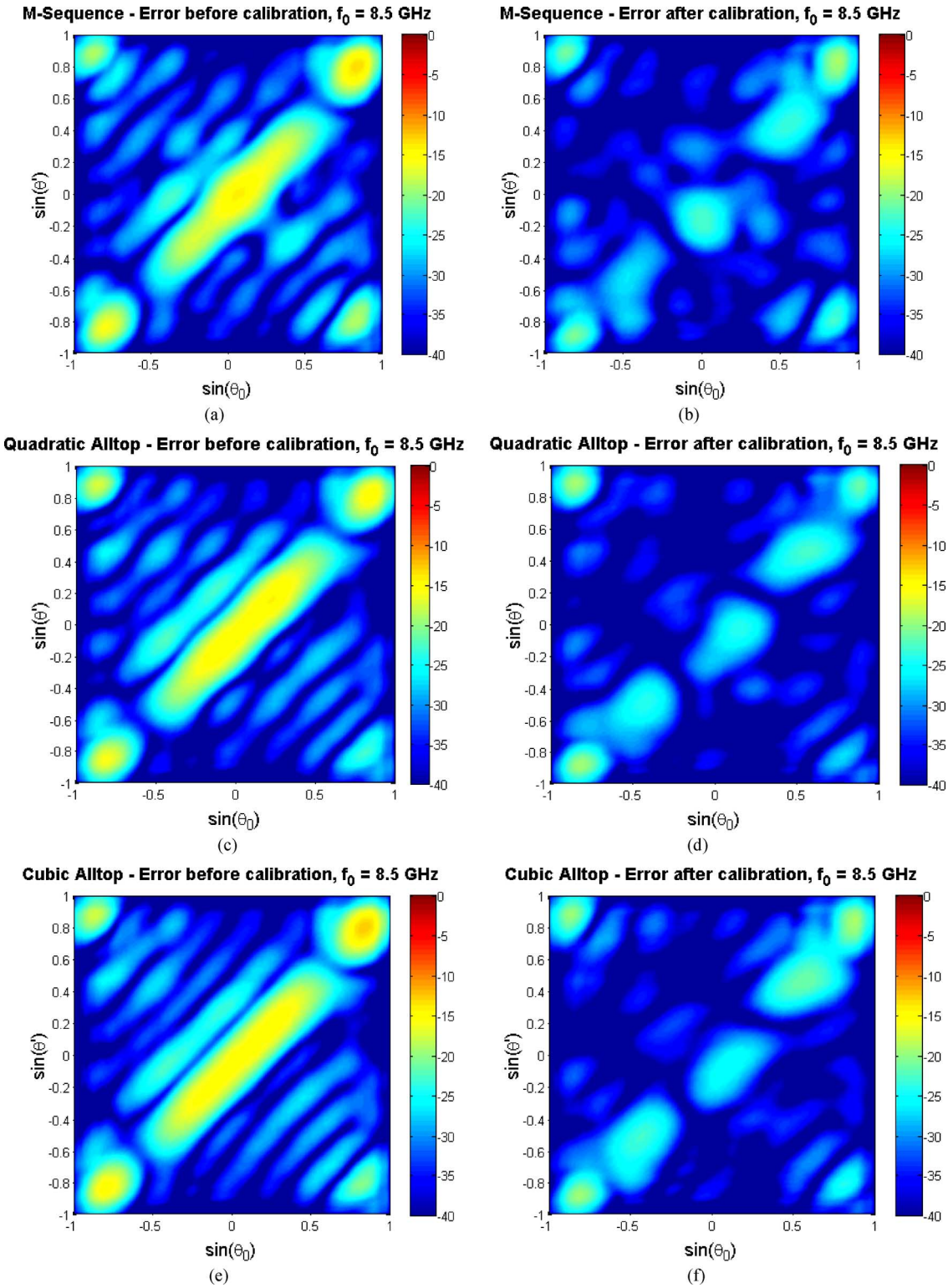

Fig. 12. Angle-angle error $\left|R^{er}_{\theta_0}(\tau'=0,\theta')\right|^2$ and for the real signals: M-sequences, cubic and quadratic Alltop sequences at 8.5 GHz and for the real antenna array before and after calibration.

since the antenna used in the experiment has been designed for 50 Ω impedance matching.

According to the antenna's specification, it can operate between 8 and 12 GHz. The antenna plate was mounted on the positioning column inside the anechoic chamber. Each of the 8 tested elements was connected to a port of the multiport switch. The network analyzer was set to sweep from 8 to 12 GHz with 401 points. 28 full 2 port calibrations for reflection/coupling

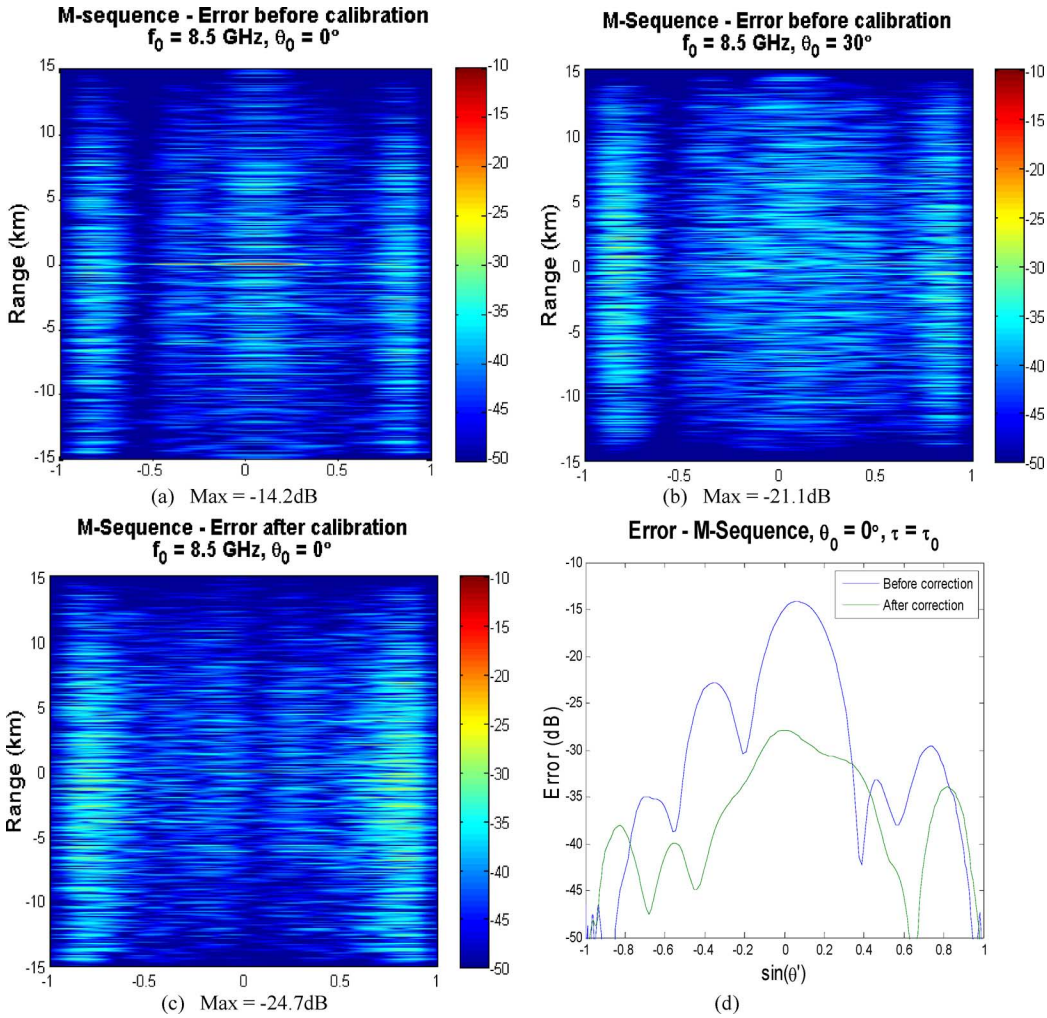

Fig. 13. Range-angle error signal $\left|R^{er}_{\theta_0=0^\circ}(\tau',\theta')\right|^2$ for M-sequences at 8.5 GHz: (a) before calibration at $\theta_0 = 0^\circ$; (b) before calibration at $\theta_0 = 30^\circ$; (c) after calibration at $\theta_0 = 0^\circ$; (d) after calibration at $\theta_0 = 0^\circ$ and $\tau = \tau_0$. (a) $\mathrm{Max} = -14.2$ dB. (b) $\mathrm{Max} = -21.1$ dB. (c) $\mathrm{Max} = -24.7$ dB.

measurements have been done. Due to the calibration, the measured coupling matrix is normalized. As an example, the measurement results for the first elements are shown in Fig. 10 as a function of frequency. Within the operating frequency band of the antenna (8.5 – 11.5 GHz) the coupling between the elements is maximal for 8.5–8.7 GHz and it is decreasing with the frequency increase, in average 2–4 dB per 1 GHz.

The measured coupling has been used for the analysis of the coupling effects on the compressed signal, provided by (15)–(17).

Fig. 11 demonstrates the angle-angle error for the beam-forming on transmit for the measured X-band antenna array, when the measured coupling and embedded elements patterns at {8.5, 9.5, 10.5, 11.5} GHz (see the example of the coupling as a function of frequency for one antenna element in Fig. 10) have been taken into account. The waveforms were assumed for the calculations to be ideally orthogonal to analyze only the coupling influence, without the interference of the signals due to the cross-correlation, which can vary with the waveform type. It can be seen that even under this assumption the beamforming on transmit is affected by the error, which is quite different for different operational frequencies of the array. So, when the sounding signals are supposed to be ideally orthogonal, the maximal error focused on the central lobe along the main diagonal, where the observed direction is equal to the beam-formed direction, $\theta' = \theta_0$, can be estimated as $\{-15, -17, -21, -23\}$ dB, see Fig. 11(a)–(d), correspondingly. We can clearly see that the decrease of the coupling between the elements with the frequency increase results in the decrease of the error value present in the analyzed ambiguity function. Apparently, we can also see that for the operating frequency 8.5 GHz the maximal error is present at the observed angles close to 90° ($\sin(\theta') = 1$). This is due to the fact that the antenna array has not been designed for operation in such a large angular sector. Anyhow, the considered array is never used for beamforming in the angular directions close to 90° or -90°. So, the analysis of the errors close to these angles is not significant.

Logically, if the error level is much smaller than the maximal sidelobe level for the ambiguity functions, namely, its angle-

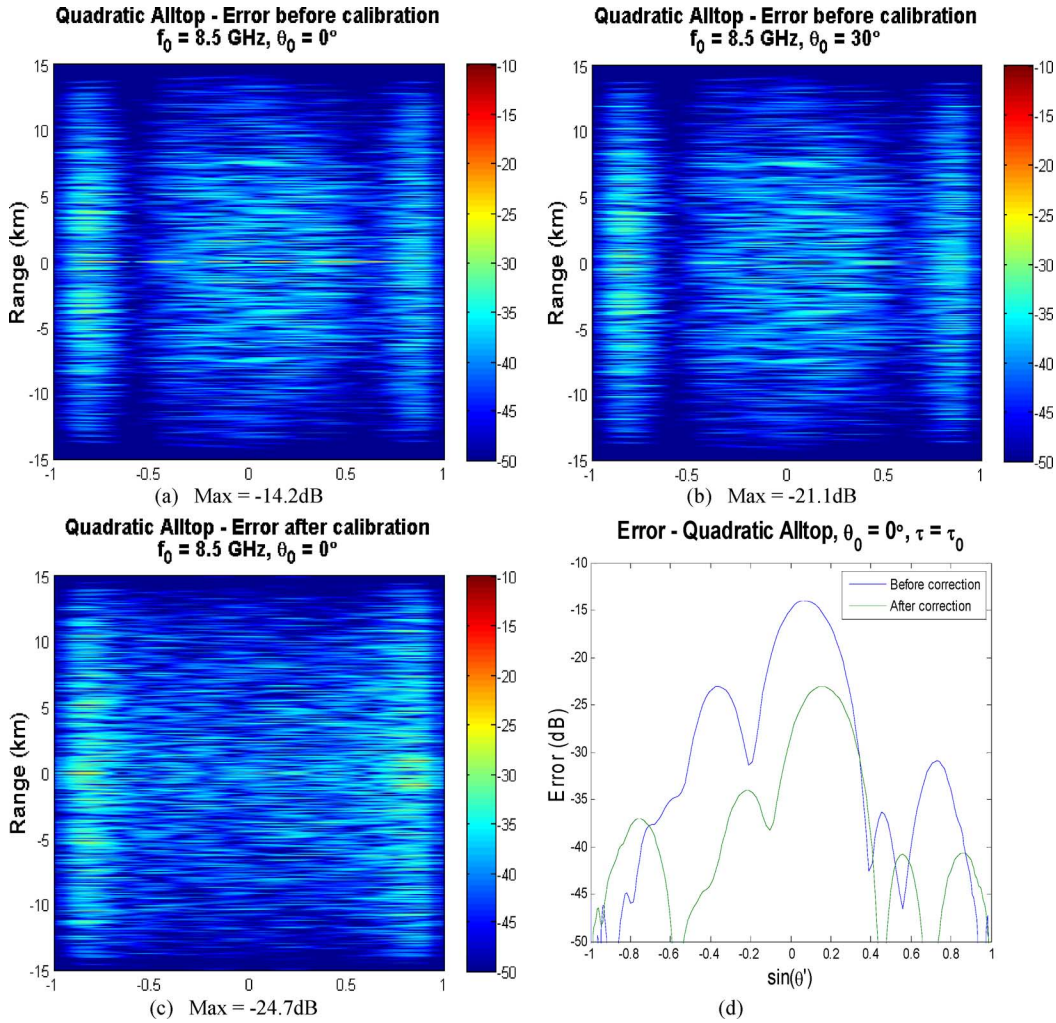

Fig. 14. Range-angle error signal $\left|R^{er}_{\theta_0=0^\circ}(\tau',\theta')\right|^2$ for Quadratic Alltop sequences at 8.5 GHz: (a) before calibration at $\theta_0 = 0^\circ$; (b) before calibration at $\theta_0 = 30^\circ$; (c) after calibration at $\theta_0 = 0^\circ$; (d) after calibration at $\theta_0 = 0^\circ$ and $\tau = \tau_0$. (a) $\mathrm{Max} = -14.2$ dB. (b) $\mathrm{Max} = -21.1$ dB. (c) $\mathrm{Max} = -24.7$ dB.

angle cuts (see, for example, the angle-angle cuts in Figs. 2–4) at a certain operation frequency, there might be no need for an error compensation at that frequency. For the demonstration of the calibration technique proposed in the previous Section the worst case among the considered ones has been chosen. The coupling between the array elements at 8.5 GHz gives the maximal error in the ambiguity function representing the possibilities of the array for beam-forming on transmit, and has to be compensated first.

Fig. 12 shows the efficiency of the calibration on transmit on the angle-angle plane for three typical space-time codes: M-sequences, quadratic and cubic Alltop sequences. Analysis of the results shows that the performances of the calibration on transmit for the different codes is quite efficient ($\sim$ 10 dB improvement) and roughly equivalent for the different codes.

Figs. 13–15 present the range-angle cuts of the error signal for M-sequences, quadratic and cubic Alltop sequences, consequently, for two implicit positions of the target, $\theta_0 = \{0^\circ, 30^\circ\}$. The error value is rather large for $\theta_0 = 0^\circ$ [Figs. 13(a)–15(a)] and comparable with the sidelobe level of the ambiguity functions, see Figs. 2–4. In contrast, the error value is rather small and there is no need for calibration on transmit for the implicit target's position $\theta_0 = 30^\circ$, Figs. 13(b)–15(b). In turn, the calibration performed on the zero angular direction, Figs. 13(c)–15(c), demonstrate $\sim$ 10 dB improvement, what can be clearly seen on the fixed range (time) parameter $\tau = \tau_0$, Figs. 13(d)–15(d).

VI. Conclusion

This paper presents a detailed analysis of antenna coupling effects on the beamforming on transmit implemented by means of signal processing in the MIMO radar receiver. The error due to these effects is illustrated first under assumption of ideally orthogonal codes and then on three typical space-time codes: M-sequences, Quadratic and Cubic Alltop codes.

A calibration technique for the beamforming on transmit (to be implemented on each receiver channel) is presented in this paper. The calibration can be performed depending on the implicit position of the target, where the error level is considered as high. The experiments with the real codes and the real X-band

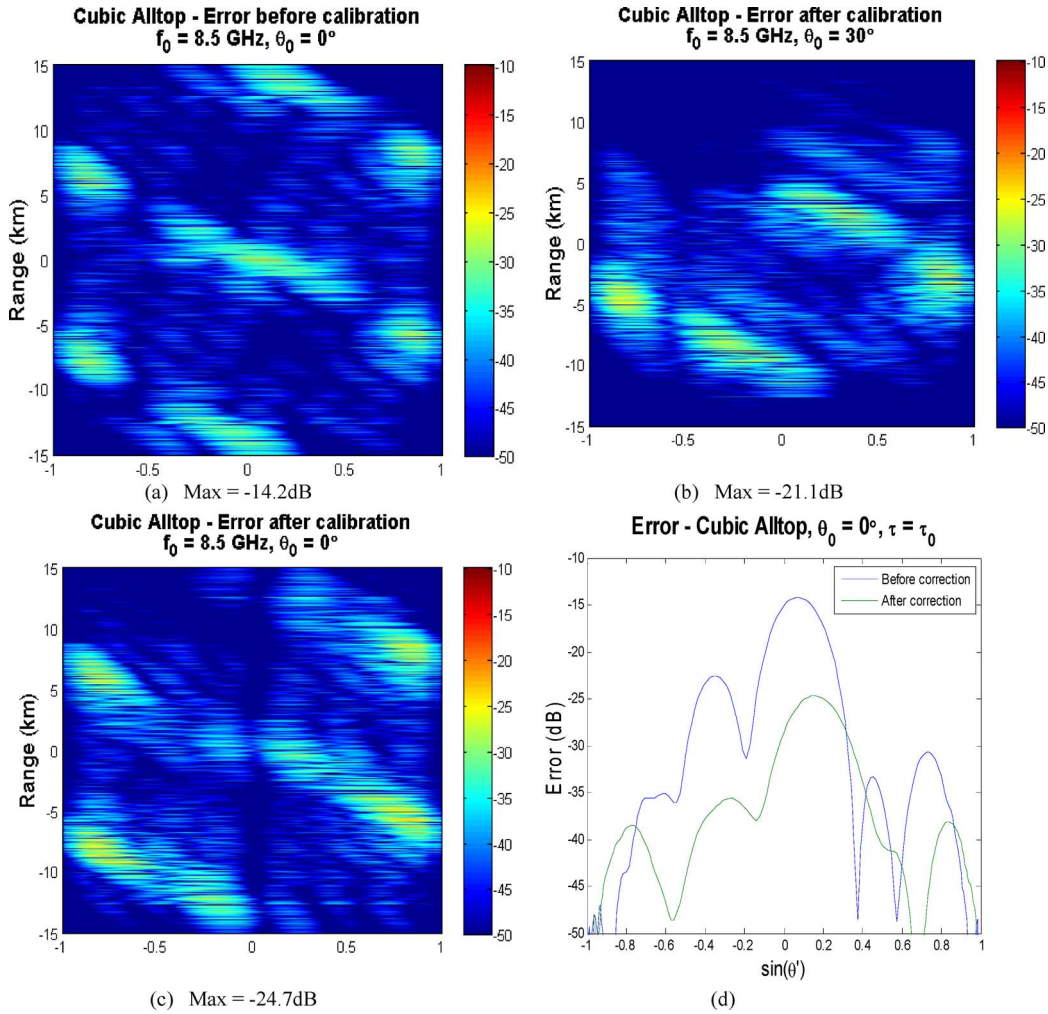

Fig. 15. Range-angle error signal $\left|R^{er}_{\theta_0=0^\circ}(\tau',\theta')\right|^2$ for Qubic Alltop sequences at 8.5 GHz: (a) before calibration at $\theta_0 = 0^\circ$; (b) before calibration at $\theta_0 = 30^\circ$; (c) after calibration at $\theta_0 = 0^\circ$; (d) after calibration at $\theta_0 = 0^\circ$ and $\tau = \tau_0$. (a) $\mathrm{Max} = -14.2$ dB. (b) $\mathrm{Max} = -21.1$ dB. (c) $\mathrm{Max} = -24.7$ dB.

antenna array have validated the coupling analysis and the efficiency of the calibration technique presented in the paper.

ACKNOWLEDGMENT

The authors would like to thank F. Wajer and S. van den Berg from Thales for valuable discussions.

REFERENCES

[1] D. J. Rabideau, "Adaptive MIMO radar waveforms," presented at the IEEE Radar Conf., RADAR '08, May 2008.

[2] *MIMO Radar Signal Processing*, J. Li and P. Stoica, Eds.. Hoboken, NJ, USA: Wiley, 2009.

[3] A. Farina, *Antenna-Based Signal Processing Techniques for Radar Systems*. Boston, MA, USA: Artech House, 1992.

[4] F. Le Chevalier, "Space-time transmission and coding for airborne radars," *Radar Sci. Technol.*, vol. 6, no. 6, Dec. 2008.

[5] F. Le Chevalier, "Space-time coding for active antenna systems," in *Principles of Modern Radar, Vol 2: Advanced Techniques*, W. L. Melvin and J. A. Sheer, Eds. Edison, NJ, USA: Scitech Publishing, an Imprint of the IET, 2013.

[6] R. Calderbank, S. D. Howard, and B. Moran, "Waveform diversity in radar signal processing," *IEEE Signal Process. Mag.*, vol. 26, no. 1, pp. 32–41, Jan. 2009.

[7] S. Drabowitch and C. Aubry, "Pattern compression by space-time binary coding of an array antenna," presented at the AGARD CP 66, Advanced Radar Syst., 1969.

[8] J. Dorey, Y. Blanchard, F. Cristophe, and G. Garnier, "Le projet RIAS, une approche nouvelle du radar de surveillance aerienne," *L'Onde Electrique*, vol. 64, no. 4, 1978.

[9] J. Jakabosky, S. D. Blunt, M. R. Cook, J. Stiles, and S. A. Seguin, "Transmitter-in-the-loop optimization of physical radar emissions," presented at the IEEE Radar Conf., Atlanta, GA, USA, May 7–11, 2012.

[10] J. Jakabosky, L. Ryan, and S. D. Blunt, "Transmitter-in-the-loop optimization of distorted OFDM radar emissions," presented at the IEEE Radar Conf., Ottawa, ON, Canada, Apr.-May 29–3, 2013.

[11] I. J. Gupta and A. K. Ksienski, "Effect of mutual coupling on the performance of adaptive arrays," *IEEE Trans. Antennas Propag.*, vol. AP-31, no. 5, pp. 785–791, May 1983.

[12] H. T. Hui, "Improved compensation for mutual coupling effect in a dipole array for direction finding," *IEEE Trans. Antennas Propag.*, vol. 51, no. 9, pp. 2498–2503, Sep., 2003.

[13] Y. Yu and T. H. Hui, "Design of a mutual coupling compensation network for a small receiving monopole array," *IEEE Trans. Microw. Theory Tech.*, vol. 59, no. 9, pp. 2241–2245, Sep., 2011.

[14] T. Sato and R. Kohno, "New calibration matrix calculation method for removing the effect of mutual coupling for uniform linear array," in *Proc. IEEE 63rd Vehicular Technology Conf.*, 2006, pp. 2686–2690.

[15] K. M. Pasala and E. M. Friel, "Mutual coupling effects and their reduction in wideband direction of arrival estimation," *IEEE Trans. Aerosp. Electron.c Syst.*, vol. 30, no. 4, pp. 1116–1122, 1994.

[16] J. A. G. Malherbe, "Analysis of a linear antenna array including the effects of mutual coupling," *IEEE Trans. Ed.*, vol. 32, no. 1, pp. 29–34, Feb. 1989.

[17] Y. Wu, J. P. Linnartz, J. W. M. Bergmans, and S. Attallah, "Effects of antenna mutual coupling on the performance of MIMO systems," presented at the 29th Symp. Inf. Theory, Benelux, May 2008.
[18] M. Hefnawi, J. Gai, and R. A. Elasoued, "Mutual coupling effects on MIMO-adaptive beamforming systems," presented at the 3rd Int. Conf. Networking and Services (ICNS'07), 2007.
[19] J. L. Alvarez-Perez and J. Pineiro-Ave, "Mutual coupling modelling in antenna arrays with the T-matrix method," presented at the 32nd ESA Antenna Workshop, Oct. 2010.
[20] G. Babur, P. Aubry, and F. Le Chevalier, "Space-time radar waveforms: Circulating codes," *J. Elect. Comput. Eng., Special Issue on "Advances in Radar Technologies"*, vol. 2013, no. Article ID 809691, p. 8.
[21] P. Calvary and D. Janer, "Spatio-temporal coding for radar array processing," in *Proc. IEEE Int. Conf. Acoust., Speech and Signal Processing*, Seattle, WA, USA, May 1998, vol. 4, pp. 2509–2512.
[22] Z. Huang and C. A. Balanis, "Mutual coupling compensation in UCAs: Simulations and experiment," *IEEE Trans. Antennas Propag.*, vol. 54, pp. 3082–3086, Nov. 2006.
[23] D. Sarwate and M. B. Pursley, "Cross-correlation properties of pseudorandom and related sequences," *Proc. IEEE*, vol. 68, no. 5, pp. 593–619, May 1980.
[24] H. Singh, H. L. Sneha, and R. M. Jha, "Mutual coupling in phased arrays: A review," *Int. J. Antennas Propag.*, vol. 2013, no. Article ID 348123, p. 23.
[25] B. Friedlander and A. J. Weiss, "Direction finding in the presence of mutual coupling," *IEEE Trans. Antennas Propag.*, vol. 39, no. 3, pp. 273–284, Mar. 1991.

Galina Babur received the M.S. degree in radioelectronic systems from the Tomsk State University of Control System and Radioelectronics (TUCSR), Russia, in 2003, and the Ph.D. degree from the Delft University of Technology (TU Delft), Delft, The Netherlands, in 2009.

In 2008, she joined the International Research Centre for Telecommunications—Transmission and Radar (IRCTR), TU Delft, The Netherlands. Since 2009, she has been a postdoctoral researcher. She specializes in signal design and signal processing for polarimetric and MIMO radars.

Pascal J. Aubry received the D.E.S.S. degree in electronics and automatics from Université Pierre et Marie Curie (Paris 6), Paris, France, in 1993.

In 1996, he was a Young Graduate Trainee with the European Space Research and Technology Centre. Since 1997, he has been with the International Research Centre for Telecommunications-Transmission and Radar (IRCTR), Delft University of Technology, Delft, The Netherlands. His interests include antenna measurement techniques, radar testing, and radar signal processing.

François Le Chevalier is Chief Scientist, Thales Land & Air Systems, and Professor, Radar Systems Engineering, Delft University of Technology (TU Delft), Delft, The Netherlands. A French pioneer in adaptive digital beamforming and STAP radar systems demonstrations, his current research activities include space-time coding for active antenna systems and wideband unambiguous radar systems. An author of many papers, tutorials, and patents in radar and electronic warfare, he is the author of a book on *Principles of Radar and Sonar Signal Processing* (Artech House, 2002), editor of *Non-Standard Antennas* (Wiley, 2010), and coauthor of *Principles of Modern Radar: Advanced Techniques* (Scitech, IET Publishing, 2012).

Prof. Le Chevalier has been active in or chairing the Technical Program Committees of most IEEE International Radar Conferences since Brest, France, 1999, and has recently chaired the Technical Program Committee of EURAD 2012, Amsterdam, The Netherlands, and will be the Honorary Chair of SEE/IEEE International Radar Conference in France, 2014.